SUMMARY REPORT FOR THE CHARACTERIZATION OF ORIGINAL GRONINGEN MASONRY

Masonry material testing 2014 and 2015

Samira Jafari and Jan Rots

TU Delft

Date December 2015

Editors Jan van Elk & Dirk Doornhof

General Introduction

To model the seismic response of Unreinforced Masonry (URM) buildings, it is important to characterise masonry material properties. This report summarises tests carried out in 2014 and 2015 on Groningen masonry by TU Delft, TU Eindhoven, and B|A|S in the laboratory and by Eucentre in-situ (Ref. 1).

The laboratory tests to determine the material parameters include: compression tests (for both the loading direction parallel and perpendicular to bed joints), flexural tests (including in-plane and out-of-plane), bond wrench tests and shear tests at different levels of confinement.

In this report, a summary is provided of the experiments. The resulting masonry properties are summarised in a summary-overview tables, where average, upper bound and lower bound values are provided.

These material properties have been used in the modelling of the seismic response of masonry index buildings in support of the development of fragility curves for masonry building typologies (Ref. 2).

References

1. In-situ testing of URM houses (building unit: Loppersum, Zijlvest 25), Eucentre, F. Graziotti, A. Rossi, I. Senaldi, S. Peloso, 5th December 2014.
2. Development of v2 fragility and consequence functions for the Groningen Field, H. Crowley, R. Pinho, B. Polidoro, P. Stafford, October 2015.

NAM

Title	**SUMMARY REPORT FOR THE CHARACTERIZATION OF ORIGINAL GRONINGEN MASONRY** **Masonry material testing 2014 and 2015**	**Date**	December 2015
		Initiator	NAM
Autor(s)	**Samira Jafari and Jan Rots**	**Editors**	Jan van Elk and Dirk Doornhof
Organisation	TU Delft	**Organisation**	NAM
Place in the Study and Data Acquisition Plan	<u>Study Theme:</u> Seismic Building response <u>Comment:</u> To model the seismic response of Unreinforced Masonry (URM) buildings, it is important to characterise masonry material properties. This report summarises tests carried out in 2014 and 2015 on Groningen masonry by TU Delft, TU Eindhoven, and B|A|S in the laboratory and by Eucentre in-situ (Ref. 1). The laboratory tests to determine the material parameters include: compression tests (for both the loading direction parallel and perpendicular to bed joints), flexural tests (including in-plane and out-of-plane), bond wrench tests and shear tests at different levels of confinement. In this report, a summary is provided of the experiments. The resulting masonry properties are summarised in a summary-overview tables, where average, upper bound and lower bound values are provided. These material properties have been used in the modelling of the seismic response of masonry index buildings in support of the development of fragility curves for masonry building typologies (Ref. 2).		
Directliy linked research	(1) Building Material properties (2) Shake table tests (3) Fragility curves for building typologies (URM) (4) Risk Assessment		
Used data	Experiments		
Associated organisation	NAM		
Assurance	TU Delft, TU Eindhoven, B|A|S and Eucentre		

Project number	C31B60
Report number	
Date	December 18, 2015
Version	2
Status	Final

SUMMARY REPORT FOR THE CHARACTERIZATION OF ORIGINAL GRONINGEN MASONRY

Masonry material testing 2014 and 2015
Client: Nederlandse Aardolie Maatschappij B.V.

Authors Samira Jafari
S.Jafari@tudelft.nl
Jan Rots
J.G.Rots@tudelft.nl
Address Delft University of Technology
Faculty of Civil Engineering and Geosciences
Stevinweg 1, 2628 CN, Delft

Table of Contents

1 Introduction

In order to carry out nonlinear finite element analysis for masonry structures, it is necessary to characterize the masonry material properties. To provide detailed information on the behaviour of Groningen masonry tests have been carried out on different types of masonry, including laboratory tests performed by TU Delft, TU/e and BAS and in-situ tests carried out by EU Centre.

Lab tests to determine the material parameters are: compression tests (for both the loading direction parallel and perpendicular to bed joints), flexural tests (including in-plane and out-of-plane), bond wrench tests and shear tests at different levels of confinement.

This report summarizes results of the lab tests and gives attention to the more exotic properties like fracture energy, shape of stress-strain relations, bending properties, and it provides correlations between the different parameters. It is a follow-up to a previous intermediate judgements of masonry properties from September 2014 and April 2015.

The report is based upon results from the following lab test series on original Groningen masonry:

- Testing campaign summer 2015 by TU Delft and TU/e [1].
- Testing campaign 2014 by TU Delft [2-12].
- Testing campaign 2014 by B|A|S: please note, only compression strength values from compression tests have been used, in section 2.1.1. All other results like Young's moduli and results from shear and tensile tests have been ignored as there was insufficient description of testing procedures, protocols and LVDT interpretations.

The resulting number of objects that formed the basis for this updated interpretation and judgement has been given for each case in the corresponding Figures.

It should be emphasized that the number of objects and masonry samples tested has increased over 2014 and 2015, but the data is still limited. The current interpretation is a step further compared to 'masonry properties 0' and 'masonry properties 1' produced before in the NAM project, but is still a judgement based on limited data and therefore subject to improvement with additional data.

2 Properties for compression

Masonry is an orthotropic material due to its special composition with individual bricks in a certain bond pattern and the special lay-out with bed joints and head joints. Often, compressive properties are specified for the vertical direction only as gravity load acts in vertical direction. However, for seismic loads we also expect horizontal compressive forces in spandrels and diagonal compressive forces. In general, constitutive models ask for properties in different directions. To serve this purpose, both vertical compression tests (load direction perpendicular to the bed joints) and horizontal compression tests (load direction parallel to the bed joints) have been carried out. This chapter presents the results in terms of compressive strength, Young's modulus, compressive fracture energy and shape of the stress-strain diagram for the two directions.

2.1 Vertical compression test

2.1.1 Vertical compression strength

Figure 1 shows the clay and calcium-silicate masonry results in terms of histograms for different intervals. The results of the lab tests, carried out by TU Delft, TU/e and B|A|S, have been considered for the preparation of histogram for clay masonry, subdivided into two age periods, before and after 1945. All delivered calcium silicate samples, tested by TU Delft and TU/e, belonged to the period before 1985.

The histogram for clay masonry displays a shift to the right side indicating higher strength with lower age. The scatter is large because of many different types of clay bricks and mortar. The results suggest some lognormal distribution. Mean values suggest 10.8 MPa for the period until 1945 and 14.3 MPa for the period after 1945. Calcium silicate units are produced in a more controlled and unified way and we observe that the scatter in calcium silicate masonry is less. Mean values suggest a compressive stress of 10.0 MPa.

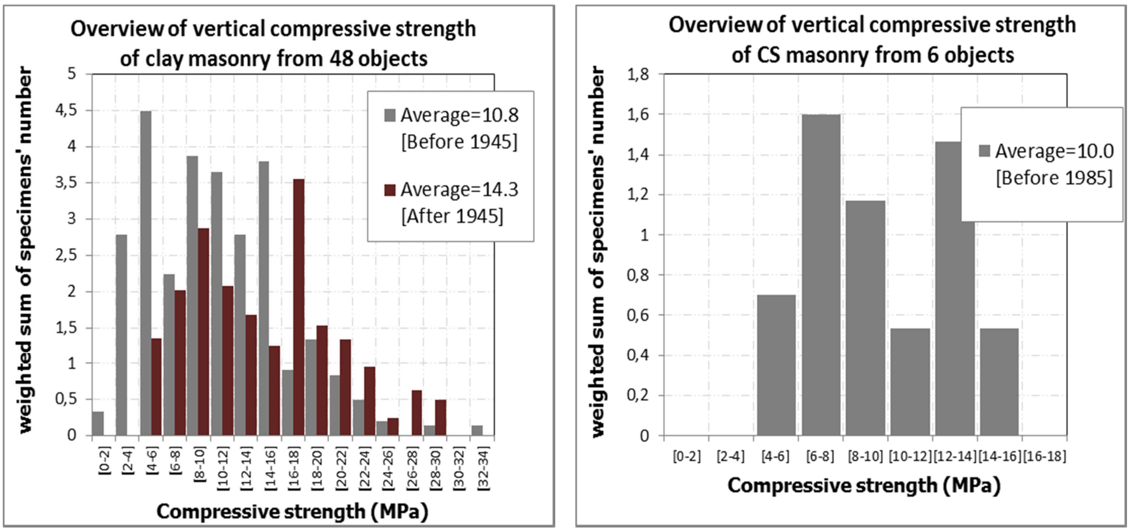

(a) (b)

Figure 1 – Histograms of vertical compressive strength: (a) all types of clay masonry; (b) calcium silicate masonry.

Figure 2 presents the histogram of vertical compressive strength for clay masonry, where the results of the tests carried out by B|A|S are excluded. It can be observed that the average values are 10.8 and 14.8 MPa, respectively, for the period before and after 1945. These values are quite similar to the average values of compressive strength when the results of tests performed by B|A|S are also taken into account (Figure 1a).

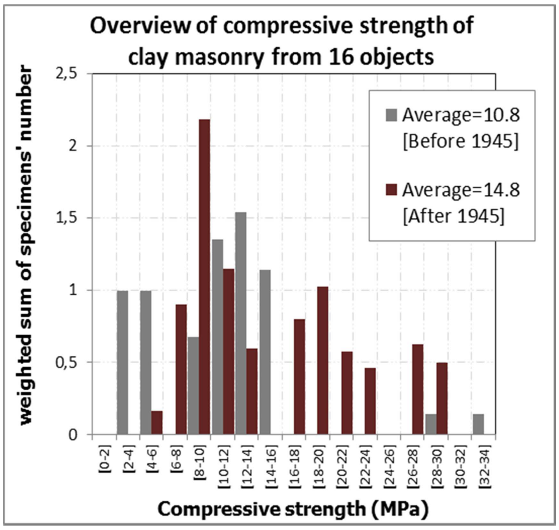

Figure 2 – Histograms of vertical compressive strength from the tests performed at TU Delft and TU/e .

2.1.2 Vertical Young's modulus

The histograms of the vertical Young's modulus calculated as the slope of the most linear part of the stress-strain curve (chord modulus) are presented in Figure 3 for both clay and calcium-silicate masonry. The chord modulus values are considered to be more realistic than the secant moduli. For secant moduli, the initial start-up of the compressive stress-strain diagram with a low slope may dominate the outcome, which is not realistic. This is also one of the reasons that B|A|S results have not been used herein. In this and all subsequent sections only results from TU Delft and TU/e have been considered for preparation of the histograms.

The histogram for clay masonry displays significant scatter in the results of Young's modulus for both periods, before and after 1945, ranging from 2 to 20 GPa. The mean values for both periods appears to be the same, 7.4 GPa.

The histogram for the Young's modulus of calcium silicate masonry shows more scatter than the histogram for the strength, which may be attributed to the variability of the mortar rather than the units, which affects deformability more than strength. Young's moduli range from 2 and 12 GPa with a mean value of 7.3 GPa.

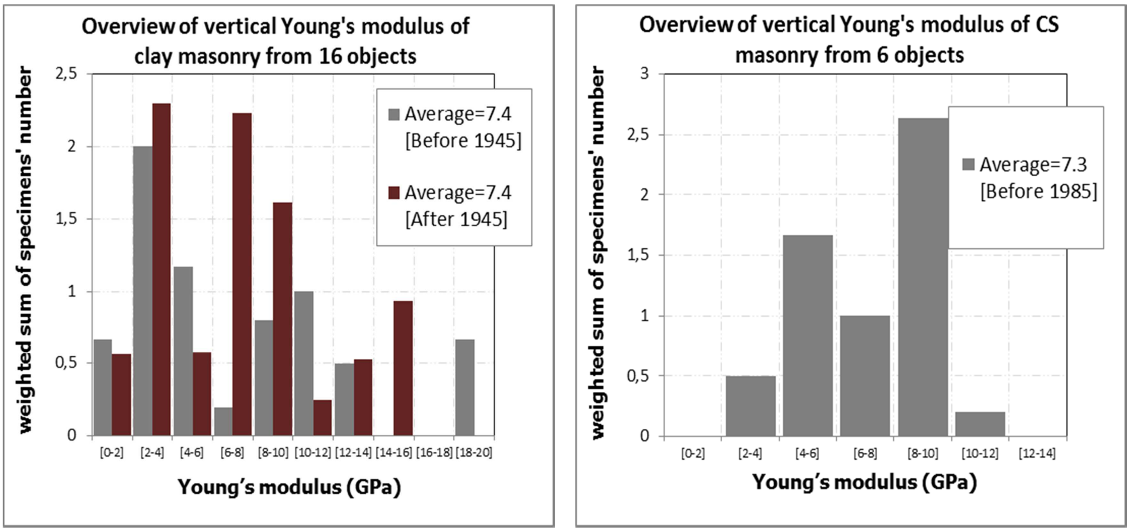

(a) (b)

Figure 3 – Histograms of vertical Young's modulus: (a) all types of clay masonry; (b) calcium silicate masonry.

2.1.3 Vertical compression fracture energy

Apart from the peak (strength) and the initial slope (Young's modulus) also the area underneath the stress-deformation curve can be used to characterize the masonry. This parameter is the compressive fracture energy. It is defined as the amount of energy consumed in the creation of all sorts of fracture surfaces in a compressed specimen over a perceived cross-sectional area of the specimen. It has been deduced from the tests carried out at TU Delft and TU/e. Figure 4 depicts the histograms of compressive fracture energy for clay and calcium-silicate masonry for the different age periods. Average values are indicated.

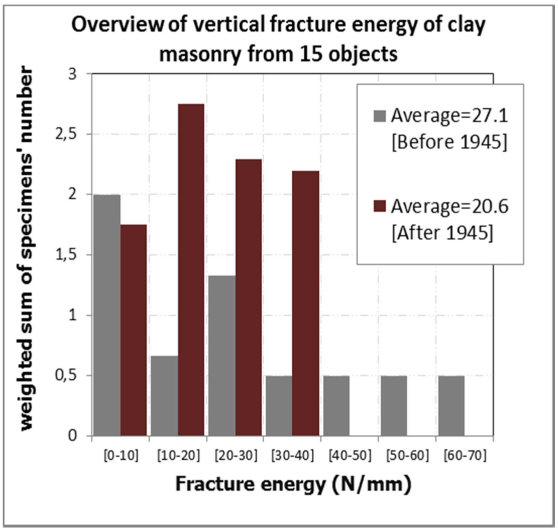

(a)

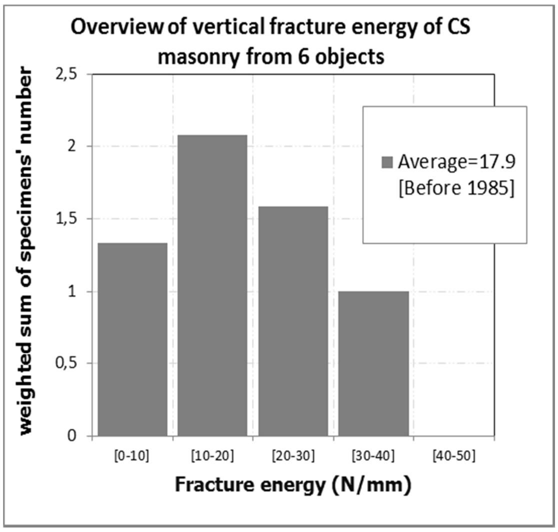

(b)

Figure 4 – Histograms of vertical compression fracture energy: (a) all types of clay masonry; (b) calcium silicate masonry.

2.2 Horizontal compression test

2.2.1 Horizontal compression strength

The results of horizontal compression tests performed at TU Delft are presented in Figure 5 in terms of histograms for clay masonry and calcium silicate masonry, categorised towards the year of construction. The histogram for clay masonry suggests that new masonry has higher strength than older masonry, as we observe a translation to the right side. Mean values suggest 9.5 MPa for the period until 1945 and 11.0 MPa for the period after 1945. The data is still limited, from 3 objects, but gives a trend. For calcium silicate masonry an average value of 6.3 MPa was found.

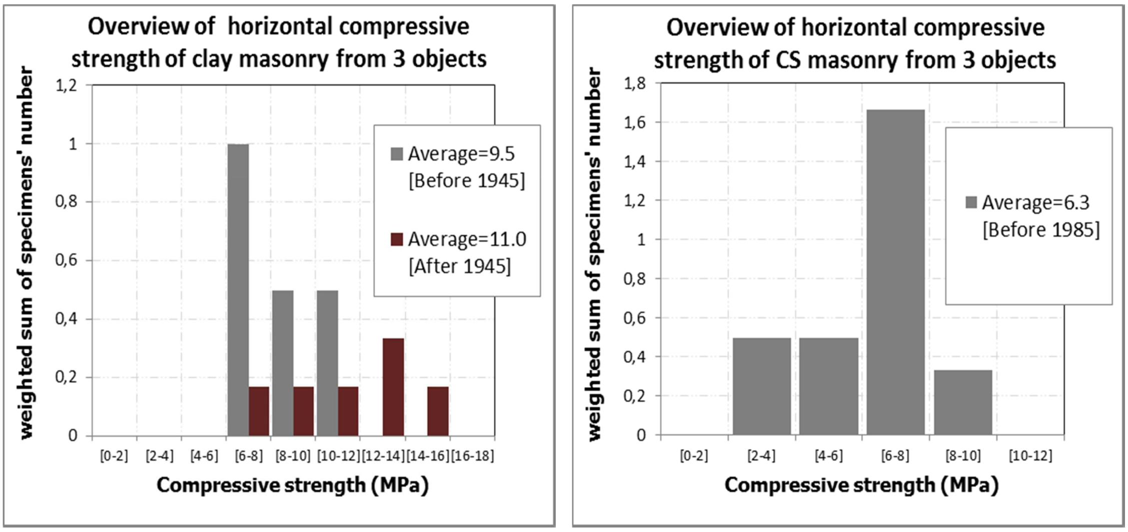

(a) (b)

Figure 5 – Histograms of horizontal compressive strength: (a) all types of clay masonry; (b) calcium silicate masonry.

2.2.2 Horizontal Young's modulus

An overview of horizontal Young's modulus values is shown in Figure 6 in terms of histograms for clay and calcium silicate masonry.

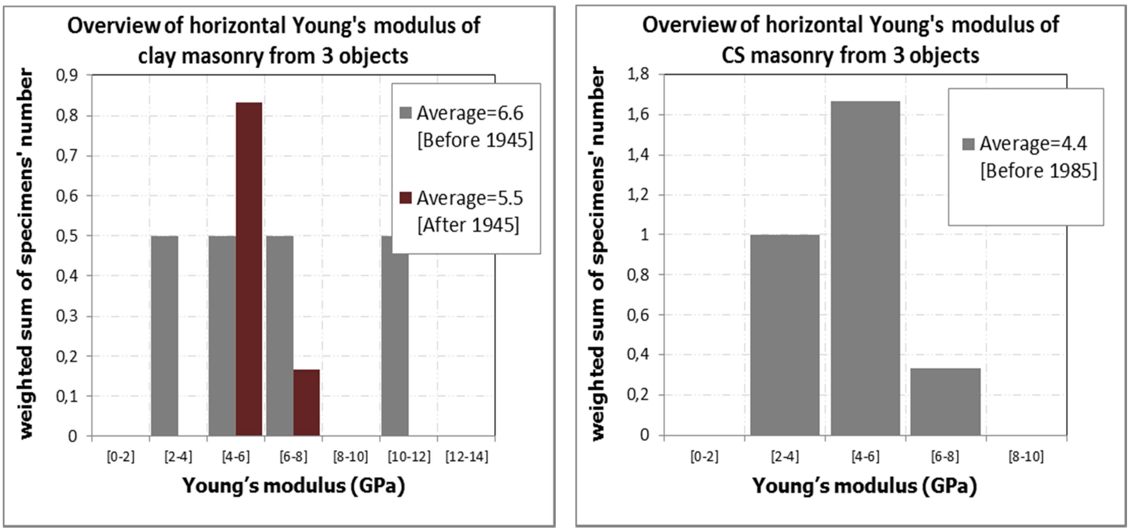

(a) (b)

Figure 6 – Histograms of horizontal Young's modulus: (a) all types of clay masonry; (b) calcium silicate masonry.

2.2.3 Horizontal compression fracture energy

The results of horizontal compression fracture energy are displayed in Figure 7 as a histogram for both clay and calcium-silicate masonry.

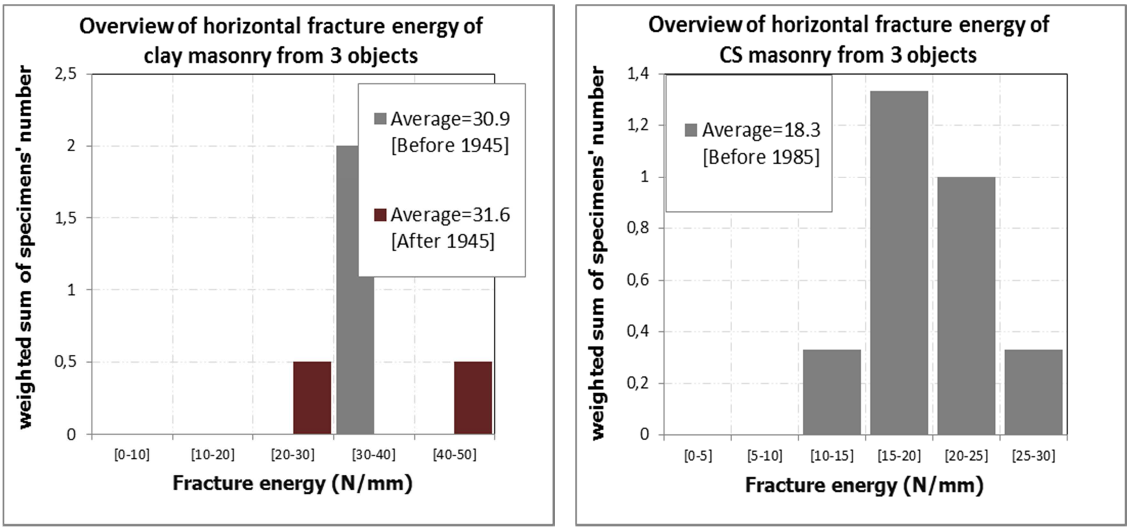

(a) (b)

Figure 7 – Histograms of horizontal compression fracture energy: (a) all types of clay masonry; (b) calcium silicate masonry.

2.3 The deformation properties of masonry in compression

Apart from the initial slope, the peak and the area underneath the diagram, also the shape of the diagram is required as an input property for hardening/softening constitutive models. As the tests at TU Delft and TU/e have been performed in displacement control, this information can be retrieved, all the way pre-peak and post-peak.

Figure 8a collects all stress-strain curves for the vertical compression tests, while Figure 8b shows again, but dimensionless, normalized towards their peak.
Figure 9a and Figure 9b represent those curves for the horizontal compression tests.

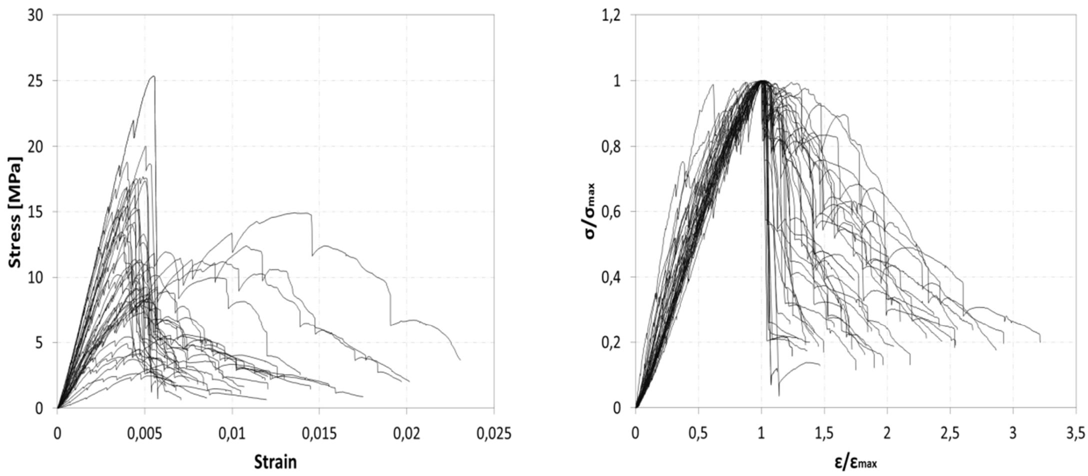

(a) (b)

Figure 8 – (a) Stress-strain curves for masonry in vertical compression tests; (b) dimensionless stress-strain curves for masonry in vertical compression tests, normalized towards the peak.

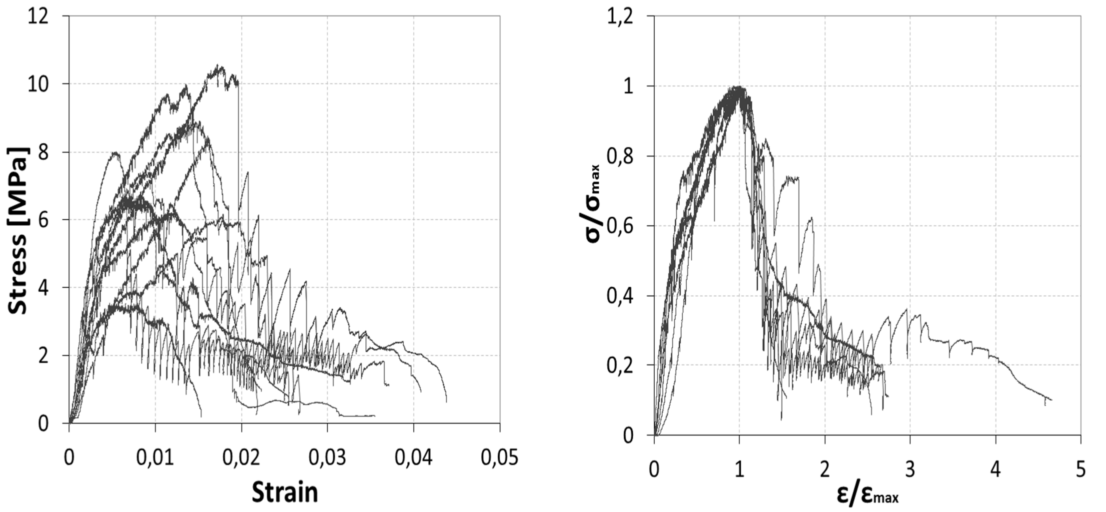

(a) (b)

Figure 9 – (a) Stress-strain curves for masonry in horizontal compression tests; (b) dimensionless stress-strain curves for masonry in horizontal compression tests, normalized towards the peak.

The average of all the normalised stress-strain curves is plotted in Figure 10 and approximated by a parabolic curve.

Well-known masonry literature (Hendry et al.) proposed the following approximation for the stress-strain curve:

$$\frac{\sigma}{\sigma_{\max}} = 2\left(\frac{\varepsilon}{\varepsilon_{\max}}\right) - \left(\frac{\varepsilon}{\varepsilon_{\max}}\right)^2 \qquad (1)$$

The agreement of the current test interpretation with this parabolic formula is remarkable. The constants for both vertical compression tests and horizontal compression tests are very close to -1.0 and 2.0.

The tail of the softening diagram from the TU Delft horizontal compressive tests shows an exponential shape. This comes close to the composite parabolic-exponential relationships curve proposed before by Lourenco & Rots (2007) and implemented in some DIANA constitutive models.

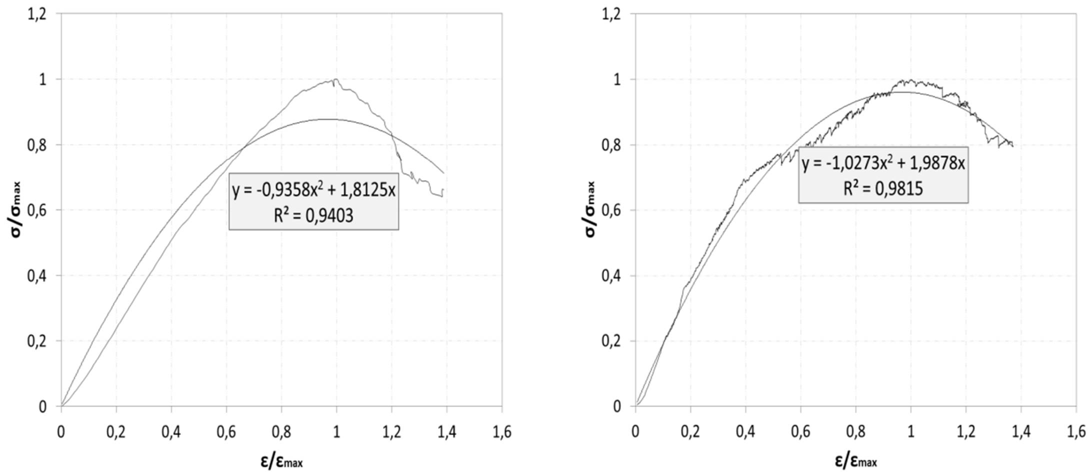

(a) (b)

Figure 10 – Average of dimensionless normalised stress-strain curves and parabolic approximation: (a) vertical compression tests; (b) horizontal compression tests.

2.4 Orthotropic effects

The laboratory tests, carried out at TU Delft (including the horizontal compression tests and the results of previous campaign) and TU/e (vertical compression tests), reveal the following conclusions: The mean compressive strength for clay brick masonry and calcium-silicate masonry dropped from 17.3 to 10.0 MPa and 10.0 to 6.3 MPa respectively, which is a reduction to 58% and 63%, respectively. The mean Young's modulus for clay brick masonry and calcium-silicate masonry dropped from 12.6 to 6.2 GPa and 7.3 to 4.4 MPa respectively, which is a reduction to 49% and 60%, respectively. The mean fracture energy for clay brick masonry and calcium-silicate masonry raised from 40.3 to 30.9 N/mm and 23.5 to 18.3 N/mm respectively.

It can be concluded that the direction of loading has a significant influence on the values of compressive strength, modulus of elasticity and fracture energy. This can be explained from the fact that the type of failure in vertical and horizontal compression tests is different. Failure of masonry wallettes in vertical compression occurred mainly by the formation of vertical cracks through bricks as a form of splitting. This obviously occurred at higher load (stronger) but was more brittle beyond peak (lower fracture energy). The elements loaded in the direction parallel to bed joints fractured mainly by delamination at bed joints. This occurred at lower load (less strong) but was more tough beyond that (higher fracture energy). Please note that size, shape and boundary effects may affect these conclusions (CUR reports 171, 191), which was not studied in the realm of this campaign.

Table 1- Ratio between vertical and horizontal compression parameters from original masonry.

Ratio	**Clay masonry**	**Calcium silicate masonry**
Vertical /Horizontal compressive strength	1.76	1.53
Vertical /Horizontal Young's modulus	2.07	1.62
Vertical /Horizontal fracture energy	1.29	1.26

Due to the limited number of tested specimens, all presented comments should be treated with care, but they give a trend. At this moment it is difficult to generalize the conclusions. However, some analogies were found with the results of related 2015 materials testing campaign for replicated masonry [13]. Table 2 shows the ratio between the compression parameters from the replicated masonry.

Table 2 - Ratio between vertical and horizontal compression parameters from replicated masonry.

Ratio	**Clay masonry**	**Calcium silicate masonry**
Vertical /Horizontal compressive strength	1.96	0.78
Vertical /Horizontal Young's modulus	1.74	1.32
Vertical /Horizontal fracture energy	1.50	0.72

2.5 Correlation between Young's modulus and compression strength

The relation between vertical Young's modulus and vertical compressive strength from TU Delft and TU/e results for clay and calcium silicate masonry are presented in Figure 11. The factor between chord Young's modulus and compression strength amounts to resp. 538 and 723 for clay masonry and calcium silicate masonry. These values are not far from prescriptions in codes, where a factor 700 is popular. For clay brick masonry the present results suggest a lower value.

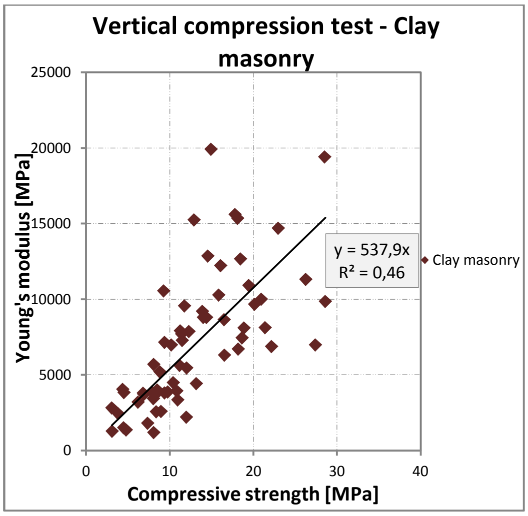

(a)

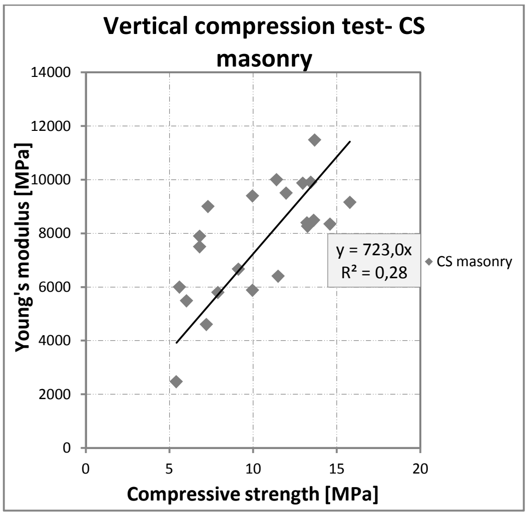

(b)

Figure 11 – Vertical Young's modulus versus vertical compressive strength: (a) clay masonry; (b) calcium silicate masonry.

Figure 12 presents the correlation between the horizontal Young's modulus and horizontal compressive strength for clay and calcium silicate masonry, respectively. Although the linear regression lines are plotted for clay and calcium silicate masonry, no correlation between compressive strength and Young's modulus can be observed. It should be mentioned that the number of the carried tests are limited to draw any conclusions.

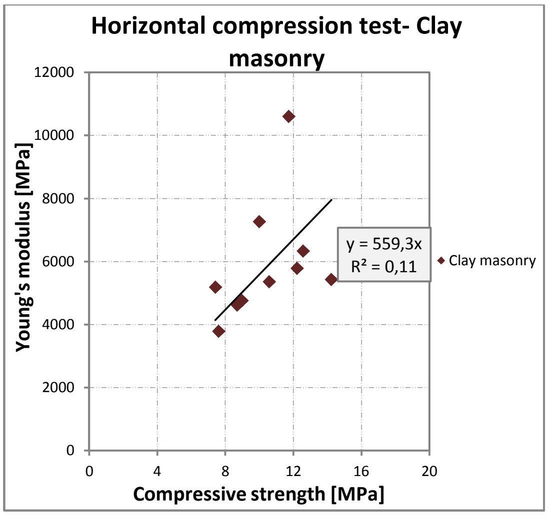

(a)

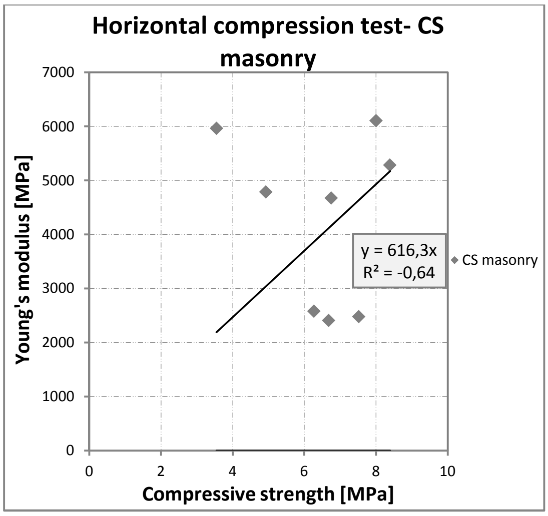

(b)

Figure 12 – Horizontal Young's modulus versus horizontal compressive strength: (a) clay masonry; (b) calcium silicate masonry.

2.6 Correlation between compression fracture energy and compression strength

Figure 13 and Figure 14 depict the correlation between the vertical compressive fracture energy and vertical compressive strength and horizontal fracture energy and horizontal compressive strength, respectively, for both clay and calcium silicate masonry. For both the clay masonry and calcium silicate masonry, linear and parabolic correlation are suggested; however, there is significant scatter and the correlations are only weak.

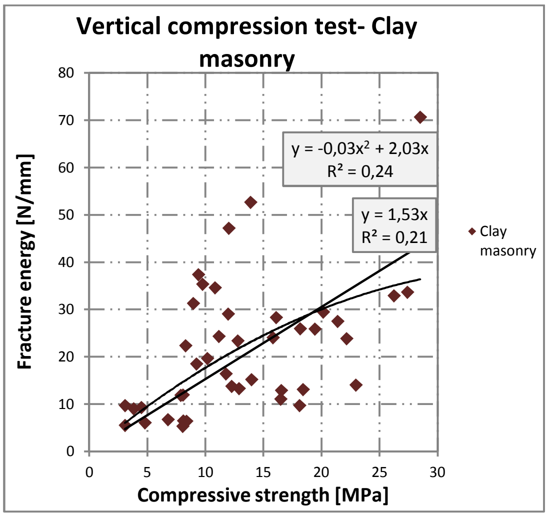

(a)

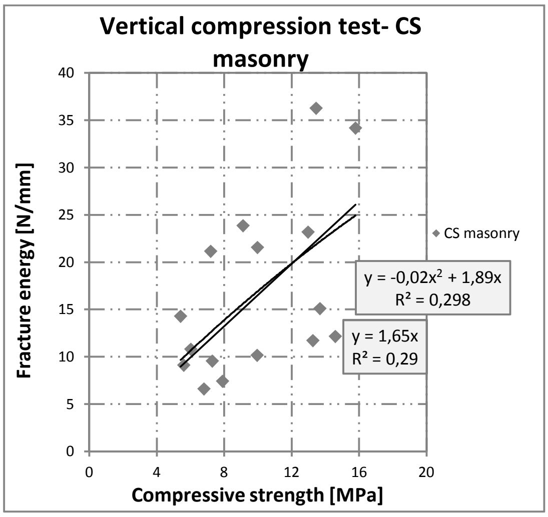

(b)

Figure 13 – Vertical fracture energy versus vertical compressive strength: (a) clay masonry; (b) calcium silicate masonry.

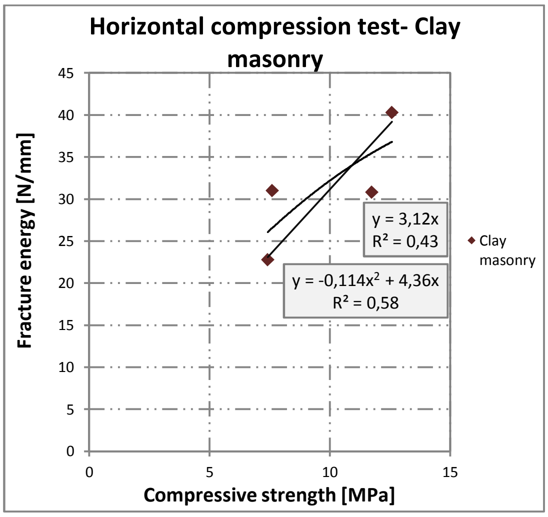

(a)

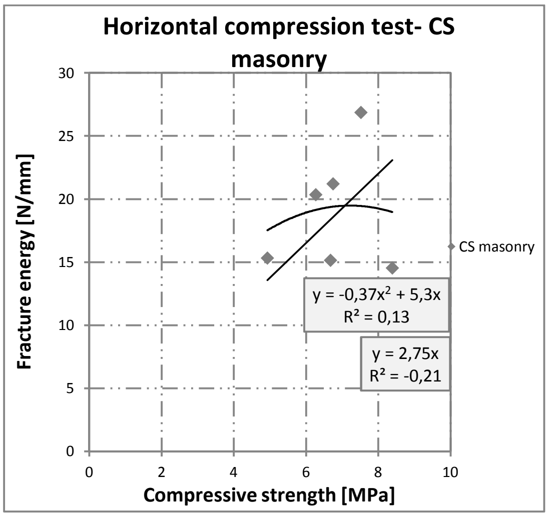

(b)

Figure 14 – Horizontal fracture energy versus horizontal compressive strength: (a) clay masonry; (b) calcium silicate masonry.

3 Properties for tension

3.1 Masonry in-plane bending tests

In-plane bending tests on masonry as a composite were carried out by TU Delft in 2014 and 2015. The tests were carried out for eleven clay masonry and five calcium silicate masonry objects. The loading direction in the four-point bending tests was taken as perpendicular to the bed joints, so that a stepped crack through head joints and bed joints or a straight crack through head joints and bricks occurs giving the f_{x3} values. The moment vector in these tests is orthogonal to the plane of the wall, horizontal bending, in-plane.

The results are displayed graphically (Figure 15), in terms of histograms for different intervals. The mean f_{x3} values for clay masonry before and after 1945 are 0.61 and 0.63 MPa, respectively. The tests on the calcium silicate masonry give a mean f_{x3} value of 0.47 MPa. It should be stated that the data for calcium silicate specimens are still very limited, since several samples arrived in such degree of disintegration that it was not possible to test them.

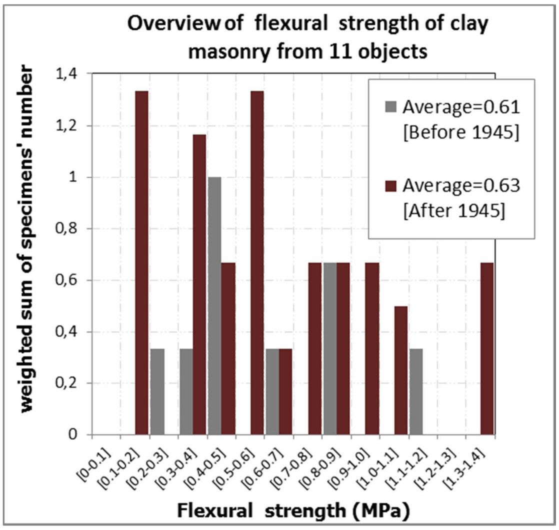

(a)

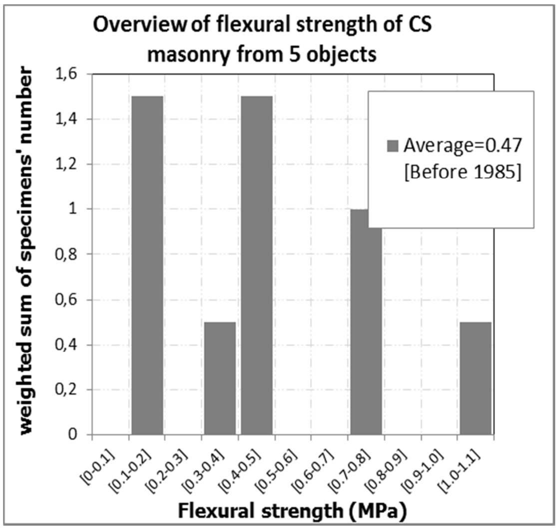

(b)

Figure 15 – Histograms of flexural strength from in-plane tests: (a) all types of clay masonry; (b) calcium silicate masonry.

3.2 Masonry out-of-plane bending tests

The tests were only carried out by TU Delft in 2014 and 2015. The loading direction was taken such that the crack plane either occurred along the head joints (giving f_{x2} values, horizontal bending, moment vector orthogonal to the bed joint and in the plane of the wall) or occurred along the brick to mortar interface in the bed joint plane (giving f_{x1} values, vertical bending, moment vector parallel to the bed joint and in the plane of the wall).

3.2.1 Vertical out-of-plane bending

The tests were carried out for eight clay masonry objects and one calcium silicate object. The results are displayed graphically (Figure 16), in terms of histograms for different intervals. The graph for all eight clay masonry objects, distinguished into two different time periods, suggests a translation to the right side indicating higher strength with lower age, although there is a need for more data to draw precise conclusions. Mean values suggest about 0.83 MPa for the period until 1945, and 1.12 MPa for the period after 1945.

It should be mentioned that calcium silicate masonry specimens were delivered at TU Delft in a degree of disintegration. As a result, there were not sufficient samples to do bending tests.

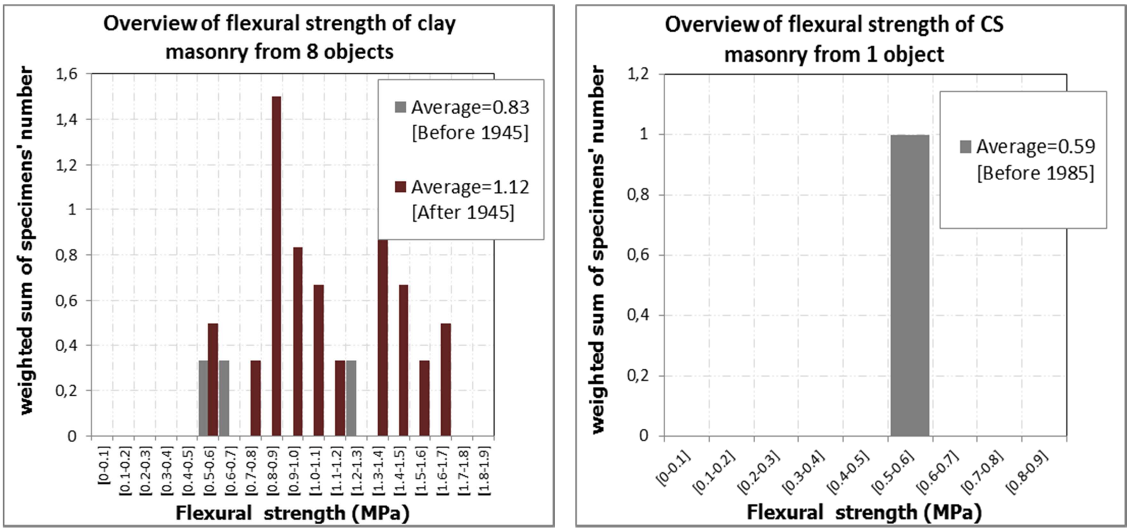

(a) (b)

Figure 16 – Histograms of flexural strength from out-of-plane tests with vertical bending: (a) all types of clay masonry; (b) calcium silicate masonry.

3.2.2 Horizontal out-of-plane bending

Figure 17 depicts histograms of clay masonry and calcium silicate masonry. The mean f_{x2} value for clay masonry from one object is 0.33 MPa, while this value for calcium silicate masonry from two objects is 0.13 MPa.
It should be stated that the data are still very limited, so a generic conclusion cannot be drawn. There is a need for further material tests to support insight in out-of-plane failure capacity, considered to be important for slender structures.

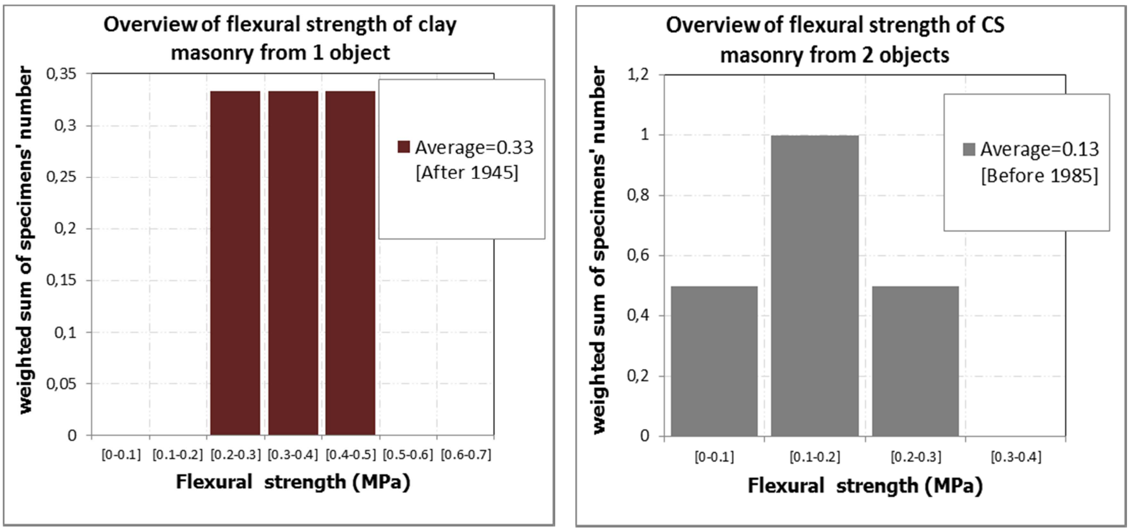

(a) (b)

Figure 17 – Histograms of flexural strength from out-of-plane tests with horizontal bending: (a) all types of clay masonry; (b) calcium silicate masonry.

3.3 Flexural bond tensile strength at brick-mortar interface

The bond wrench test provides the flexural tensile strength at the brick-mortar interface. The clay and calcium silicate masonry results of TU Delft are presented graphically in Figure 18, in terms of histograms for different intervals, as well as different time periods.
Histograms indicate that there is a significant scatter of bond strength values, both for clay and calcium silicate masonry. This confirms the general findings that the bond between mortar and brick is a

delicate issue, depending on many factors such as workmanship, the unit rate of suction, ageing, and weather during construction and so forth.
The mean values of flexural tensile bond strength for clay masonry before and after 1945 are 0.38 and 0.32 MPa, respectively. For calcium silicate masonry, which is known to have poorer bond because of e.g. water suction from the fresh mortar into the dry bricks, the mean value is only 0.11 MPa.

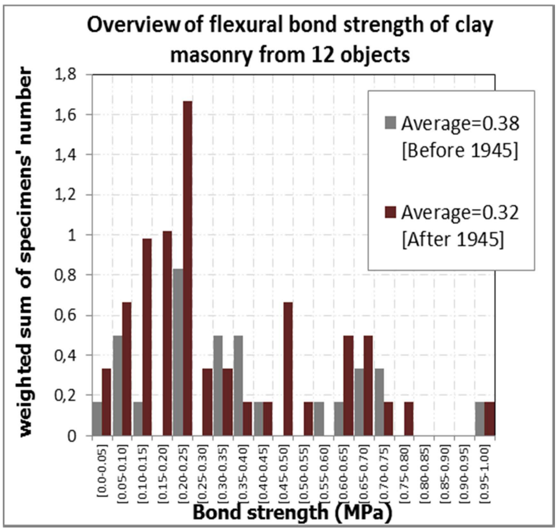

(a)

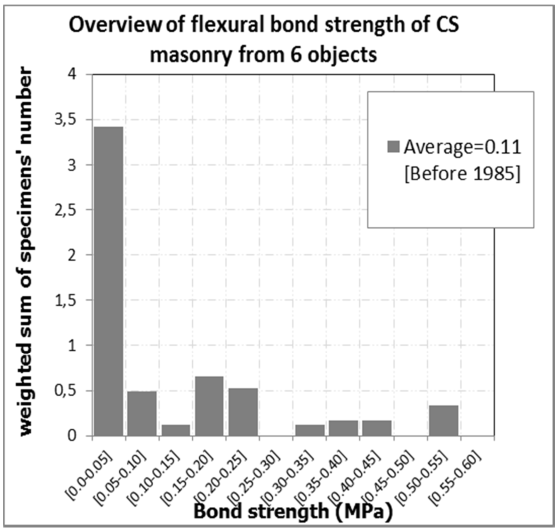

(b)

Figure 18 – Histograms of flexural bond tensile strength: (a) all types of clay masonry; (b) calcium silicate masonry.

3.4 Correlations

The average results of the ratio between different tension parameters are displayed in Table 3.

Table 3- Ratio between tension parameters from tests on original masonry.

Ratio	Clay masonry	Calcium silicate masonry
f_{x2}/ f_{x1}	2.8	4.2
f_{x3}/ f_{x1}	1.0	4.8
f_b / f_{x3}	0.5	0.6
f_b/ f_{x1}	0.6	2.0

Clearly, f_{x2} values are larger than f_{x1} as the crack runs through head joints and bed joints or head joints and bricks, which gives more resistance than just cracking a bed joint. Also for clay brick the f_{x3} value is larger than f_{x1} which is because a stepped in-plane crack through head and bed joints and/or bricks gives more resistance than just cracking a bed joint. For calcium-silicate a lower value was found, but the data was very limited.

From a physical point of view, it may be expected that there is a correlation between the flexural bond strength (f_b) and flexural masonry strength when the loading direction was taken such that the crack plane occurred along the brick to mortar interface in the bed joint plane (f_{x1}). This is because these parameters both depend on the adhesion between mortar and brick. Table 3 shows that the values are not equal, i.e. the ratio is not 1.0, for clay f_{x1} is larger than f_b while for calcium silicate f_{x1} is smaller than f_b.

Again, it should be stated that the data are still limited (especially data from out-of-plane tests), generic conclusions cannot be drawn, just first trends are indicated.

TU Delft also performed series of tests on replicated masonry, both on replicated perforated clay and replicated calcium silicate masonry. Table 4 shows the ratio between tension parameters for the replicated masonry [13]. It can be seen that there is a fair agreement between replicated masonry results and results from original masonry.

Table 4 - Ratio between tension parameters from tests on replicated masonry at TU Delft.

Ratio	**Clay masonry**	**Calcium silicate masonry**
f_{x2}/ f_{x1}	2.8	3.6
f_{x3}/ f_{x1}	1.5	1.9
f_{b} / f_{x3}	0.4	0.7
f_{b}/ f_{x1}	0.7	1.3

4 Properties for shear

4.1 Shear-compression test

TU Delft and TU/e performed shear tests at different levels of confinement, including fifteen clay masonry objects and six calcium silicate masonry objects.

An overview of all results in terms of measured initial shear strength (cohesion) is given in Figure 19 for clay masonry distinguished towards time periods and calcium silicate masonry.

The trend of bond shear strength values with different time periods of the masonry is similar to the other parameters, such as compressive strength. The older masonry on average shows lower values.

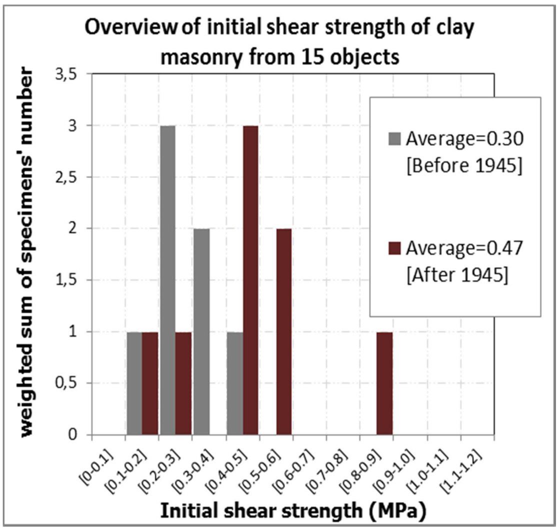

(a)

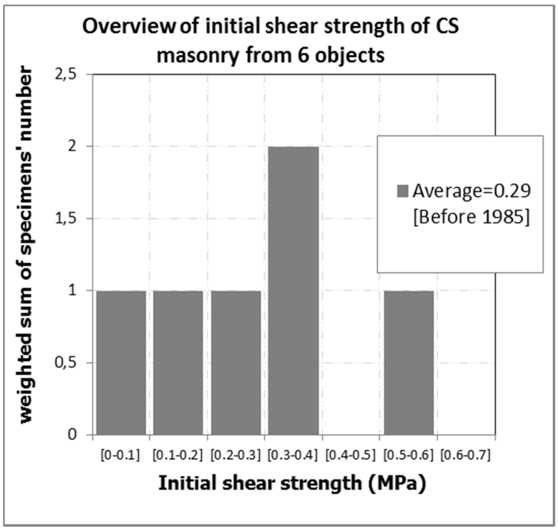

(b)

Figure 19 – Histograms of initial shear strength: (a) all types of clay masonry; (b) calcium silicate masonry.

4.2 Mode - II shear fracture energy

The mode-II shear fracture energy is area under the shear stress versus shear slip diagram, measured between the peak and the residual plateau. An example of a shear stress-displacement curve from the tests performed at TU/e and TU Delft is presented in Figure 20. The curves show an ascending branch, representing the initial elastic stage, a peak representing the initiation of bond shear fracture, a softening stage representing mode-II shear softening up to a final plateau representing residual dry friction.

The values obtained for the mode II fracture energy are presented in Figure 21, as a function of the normal stress, for both clay and calcium silicate masonry. The linear regression lines clearly show that the mode II fracture energy increases with increasing normal stress. The value of the correlation coefficient of the regression line is low, for both clay and calcium silicate masonry, and consequently it can only be considered as a first indication of the trend.

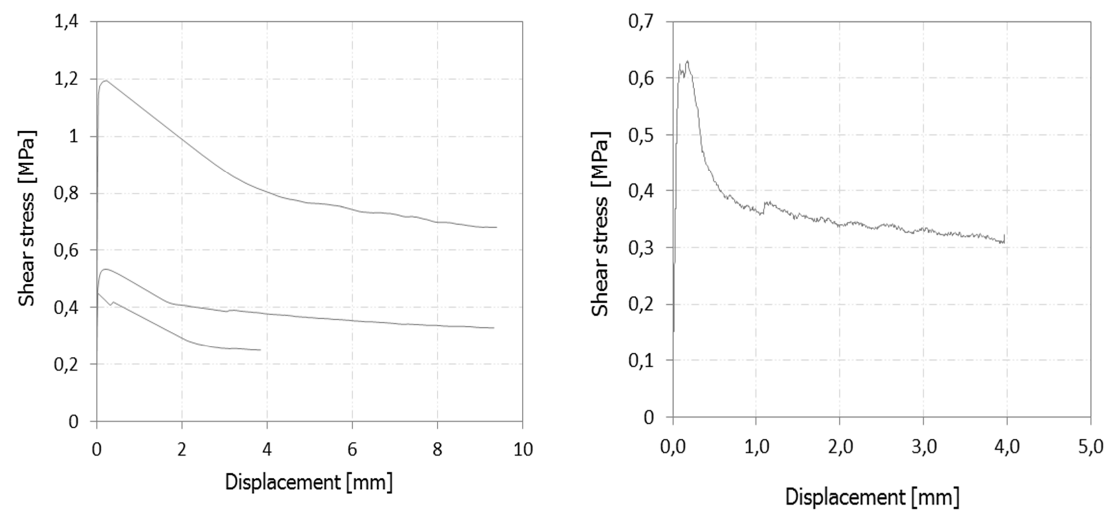

(a) (b)

Figure 20 – Shear stress-displacement curves: (a) tests performed at TU/e at the different levels of confinement; (b) tests performed at TU Delft.

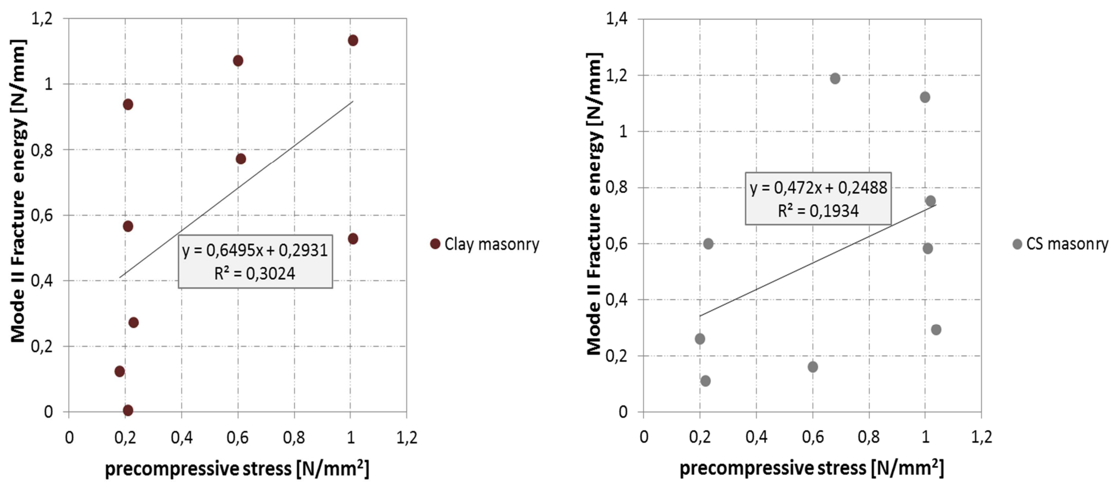

(a) (b)

Figure 21 – Mode II fracture energy of specimens as a function of the normal stress: (a) clay masonry ;(b) calcium silicate masonry.

4.3 Correlation

It may be expected that there is a correlation between bond shear and bond (uniaxial) tensile strength, since these parameters depend on the adhesion between mortar and brick. According to fracture mechanics for a propagating crack in softening material, the uniaxial bond tensile strength will be lower than the flexural bond tensile strength. Previous research has indicated that the ratio is 2/3. It should be mentioned that in nonlinear FEM analysis the uniaxial strength should be used instead of the flexural strength.

Figure 22 shows the ratio between the cohesion and the derived uniaxial tensile bond strength of joints as a function of the uniaxial tensile bond strength. It can be seen that the ratio between the cohesion and the tensile bond strength varies between 0.75 and 8.4. It can also be observed that high ratios occur when the tensile bond strength is low. Explanations have been given before in the April document. Some possible approximations of the trend are indicated, as a constant, a linear and power function. The constant factor 2, i.e. cohesion is 2 times the uniaxial tensile bond strength, fairly resembles previous estimations for fresh masonry [14]. The mentioned ratio from the tests performed on the replicated masonry is 0.77 for the clay masonry, and is 0.83 for the calcium silicate masonry [13].

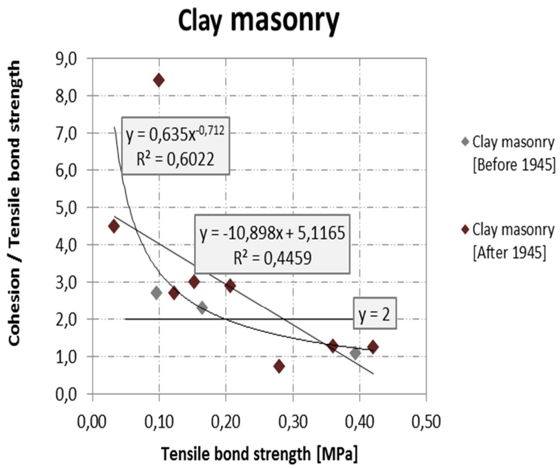

Figure 22 – Ratio between the cohesion and tensile bond strength of joints as a function of the tensile bond strength.

5 Summary-overview of material properties

The material properties, based upon the previous campaigns, are summarised in Table 5 in terms of weighted average value and coefficient of variation as well as the lower and upper bound.

Table 5 – Overview of mechanical properties based upon the all test series.

Material property	Symbol	Unit	Clay								Calcium Silicate				Concrete Block				Aerated Concrete				CS element			
			(pre 1945)				(post 1945)				(pre 1985)															
			Average	Lower bound	Upper bound	C.o.V.	Average	Lower bound	Upper bound	C.o.V.	Average	Lower bound	Upper bound	C.o.V.	Average	Lower bound	Upper bound	C.o.V.	Average	Lower bound	Upper bound	C.o.V.	Average	Lower bound	Upper bound	C.o.V.
Flexural strength of masonry unit	$f_{mu,t}$	MPa	6.43	0.71	17.35	0.53	4.29	1.30	8.79	0.41	4.26	1.16	8.36	0.11	1.27	0.37	2.39	0.61	-	-	-	-	-	-	-	-
Compressive strength of masonry in the direction perpendicular to bed joints	$f_{m,v}$	MPa	10.76	1.30	32.40	0.42	14.31	4.50	28.60	0.42	9.96	5.42	15.78	0.33	5.57	4.60	6.12	0.15	3.77	2.88	4.62	0.19	-	-	-	-
Elastic chord modulus of masonry in the direction perpendicular to bed joints	$E_{m,v}$	GPa	7.44	1.27	19.92	0.66	7.35	1.20	15.60	0.50	7.31	2.48	11.48	0.27	5.23	4.69	5.68	0.10	1.81	1.56	2.11	0.15	-	-	-	-
Fracture energy in compression for loading perpendicular to bed joints	$G_{f\text{-}c,v}$	N/mm	27.06	5.53	70.64	0.77	20.58	5.29	37.37	0.46	17.89	6.60	36.27	0.55	9.90	9.70	10.88	0.09	11.11	10.88	11.32	0.02	-	-	-	-
Compressive strength of masonry in the direction parallel to bed joints	$f_{m,h}$	MPa	9.51	7.60	11.73	0.20	11.00	7.41	14.23	0.23	6.26	3.55	8.39	0.28	-	-	-	-	2.18	1.17	2.96	0.42	-	-	-	-
Elastic chord modulus of masonry in the direction parallel to bed joints	$E_{m,h}$	GPa	6.56	3.78	10.60	0.51	5.47	4.76	6.33	0.10	4.40	2.41	6.10	0.23	-	-	-	-	0.88	0.58	1.12	0.32	-	-	-	-
Fracture energy in compression for loading parallel to bed joints	$G_{f\text{-}c,h}$	N/mm	30.94	30.84	31.04	0.005	31.55	22.80	40.30	0.39	18.34	14.54	26.89	0.15	-	-	-	-	6.96	5.30	10.00	0.38	-	-	-	-
Average of compressive strength in vertical and horizontal direction	f_m	MPa	10.13				12.65				8.11				5.57				2.97				-			
Average of elastic chord modulus in vertical and horizontal direction	E_m	GPa	7.00				6.41				5.86				5.23				1.34				-			
Average of fracture energy in vertical and horizontal direction	$G_{f\text{-}c}$	N/mm	29.00				26.07				18.12				9.90				9.04				-			
Masonry shear modulus	G_m	GPa	2.92				2.67				2.44				2.18				0.56				-			
Masonry bending strength with the moment vector parallel to the bed joints and in the plane of the wall	f_{x1}	MPa	-	-	-	-	0.33	0.26	0.42	0.24	0.13	0.00	0.28	0.17	-	-	-	-	-	-	-	-	-	-	-	-
Masonry bending strength with the moment vector orthogonal to the bed joint and in the plane of the wall	f_{x2}	MPa	0.83	0.55	1.28	0.47	1.12	0.59	1.68	0.27	0.59	0.59	0.59	-	-	-	-	-	0.47	0.44	0.50	0.09	1.29	1.20	1.38	0.10
Masonry bending strength with the moment vector orthogonal to the plane of the wall	f_{x3}	MPa	0.61	0.29	1.12	0.20	0.63	0.11	1.40	0.57	0.47	0.13	1.06	0.62	0.31	0.28	0.33	0.09	0.58	0.50	0.69	0.17	0.87	0.47	1.44	0.58
Masonry flexural bond strength between brick and mortar	$f_{b,bj}$	MPa	0.38	0.03	1.00	0.57	0.32	0.00	0.95	0.72	0.11	0.00	0.55	-	0.23	0.13	0.47	0.56	-	-	-	-	-	-	-	-
*Masonry uniaxial bond strength between brick and mortar	f_b	MPa	0.25	0.02	0.67	0.38	0.21	0.00	0.64	0.42	0.07	0.00	0.37	-	0.15	0.09	0.31	0.37	-	-	-	-	-	-	-	-
Masonry (bed joint) initial shear strength	f_{v0}	MPa	0.30	0.17	0.43	0.29	0.47	0.15	0.84	0.46	0.29	0.03	0.53	0.62	0.39	-	-	-	-	-	-	-	-	-	-	-
Masonry (bed joint) shear friction coefficient	μ	-	0.80	0.50	1.23	0.37	0.76	0.45	1.12	0.30	0.78	0.53	1.10	0.24	0.94	-	-	-	-	-	-	-	-	-	-	-
**Fracture energy in shear	$G_{f\text{-}s}$	N/mm	0.33				0.93				0.49				-				-				-			
***Fracture energy in tension	$G_{f\text{-}t}$	N/mm	0.035				0.035				0.015				-				-				-			

* According to fracture mechanics, the uniaxial bond strength is 2/3 of the flexural bond strength.
** Calculated as the average values of fracture energy at the pre-compressive stress of 0.6 MPa.
*** Derived from the previous reports.

References

[1] Jafari, S., J.G. Rots and L. Panoutsopoulou, Tests for the characterization of original Groningen masonry, Delft University of Technology, Dept. Structural Engineering, 23 October 2015.

[2] Braam, C.R. and Jafari, S, Appingedam school masonry – Compressive strength. Research report 25.5-15-07, Delft University of Technology, Dept. Structural Engineering, April 2015.

[3] Braam, C.R. and Jafari, S. Appingedam school masonry – Flexural tensile strength. Research report 25.5-15-09, Delft University of Technology, Dept. Structural Engineering, April 2015.

[4] Braam, C.R. and Jafari, S. Appingedam school masonry – Bed joint shear strength at transverse compressive stress. Research report 25.5-15-06, Delft University of Technology, Dept. Structural Engineering, 9 April 2015.

[5] Braam, C.R. and Jafari, S. Appingedam school masonry – Bond strength. Research report 25.5-15-08, Delft University of Technology, Dept. Structural Engineering, April 2015.

[6] Braam, C.R. and Jafari, S. Zijlvest house masonry - Compressive strength. Research report 25.5-15-01, Delft University of Technology, Dept. Structural Engineering, 16 March 2015.

[7] Braam, C.R. and Jafari, S. Zijlvest house masonry – Flexural tensile strength. Research report 25.5-15-04, Delft University of Technology, Dept. Structural Engineering, 9 March 2015.

[8] Braam, C.R. and Jafari, S. Zijlvest house masonry – Bed joint shear strength at transverse compressive stress. Research report 25.5-15-03, Delft University of Technology, Dept. Structural Engineering, 9 March 2015.

[9] Braam, C.R. and Jafari, S. Zijlvest house masonry – Bond strength. Research report 25.5-15-02, Delft University of Technology, Dept. Structural Engineering, 9 March 2015.

[10] Braam, C.R. and Jafari, S, Zijlvest house material – Flexural bending strength and compressive strength of bricks. Research report 25.5-15-05, Delft University of Technology, Dept. Structural Engineering, 9 March 2015.

[11] Rots, J.G. and Jafari, S. Conclusive summary report – Masonry material testing 2014, Delft University of Technology, Dept. Structural Engineering, 13 April 2015.

[12] Rots, J.G. and Jafari, S. Overview of TU Delft and B|A|S results. Technical note, Delft University of Technology, Dept. Structural Engineering, intermediate version, 18 February 2015

[13] Esposito, R., F. Messali, Crielaard, R. and J.G. Rots, Tests for the characterization of replicated masonry, Delft University of Technology, Dept. Structural Engineering, 23 October 2015.

[14] CUR rapport 171, Constructief metselwerk – een experimenteel/numerieke basis voor praktische rekenregels. CUR Civieltechnisch Centrum Uitvoering Research en Regelgeving, Gouda, 1994. Also published in English: Structural Masonry – an experimental/numerical basis for practical design rules, A.A. Balkema, Rotterdam/Brookfield, 1997.

Appendix A

Resulting from intermediate project communications and in order to further investigate the correlations between the mechanical properties of the masonry, it was proposed to subdivide data into the year of the construction, type of the brick and the quality. In this respect, the clay and calcium silicate masonry are categorised into the years before and after 1945 and 1985, respectively, while the clay brick masonry is categorised into the type of the brick such as the solid, perforated and frogged unit. Moreover, each object is divided into the "Good quality" or "Poor quality", based on the field observations considering the quality of the mortar, filling of the joints and the layout. It is worthy to note that categorizing data based on the quality is not always supported by the results of the in-situ tests such as penetrometric tests (by which the quality of the mortar was investigated).

Figure 23 shows the values of the vertical Young's modulus versus vertical compressive strength for both the clay and calcium silicate masonry specimens. Clay brick specimens are categorised into the year of the construction, type of the brick and quality, while calcium silicate specimens are categorised into the year of the construction and quality. Although the linear regression lines are plotted for each subcategory, no clear trend or conclusion can be drawn yet from the categorized data.

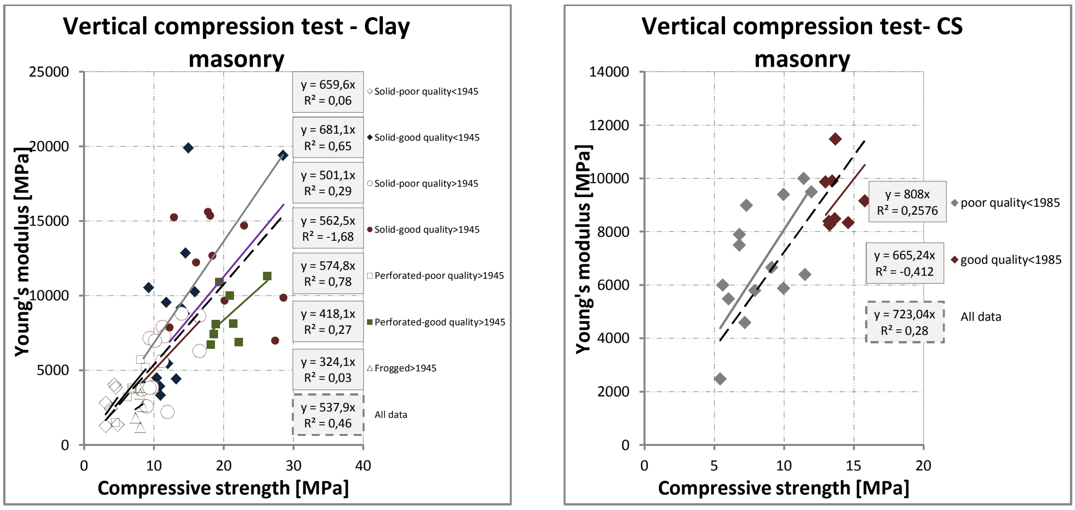

(a) (b)

Figure 23 – Vertical Young's modulus versus vertical compressive strength: (a) clay masonry; (b) calcium silicate masonry.

Figure 24 presents the values of the horizontal Young's modulus versus the horizontal compressive strength for both the clay and calcium silicate masonry. As mentioned before the data is still too limited to draw general conclusions.

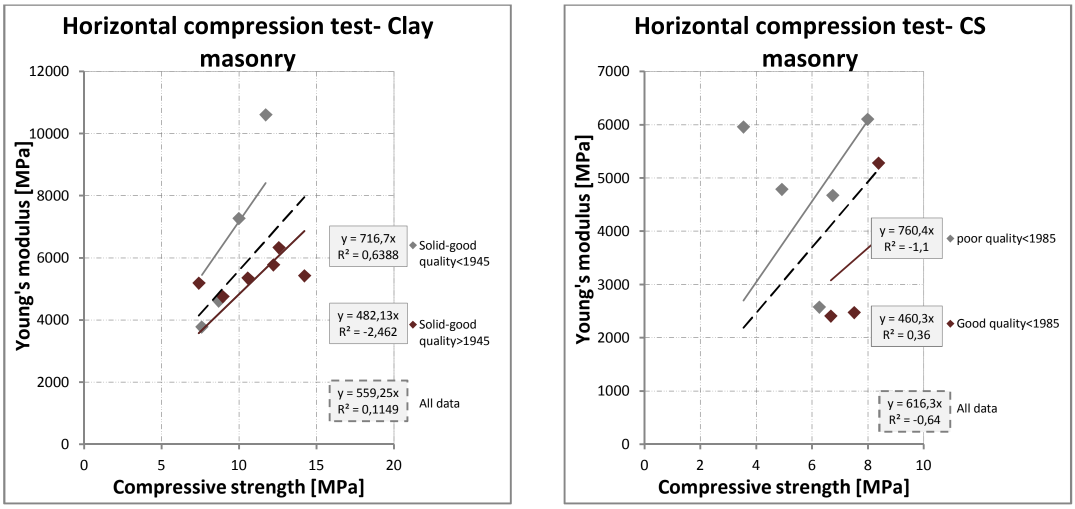

(a) (b)

Figure 24 – Horizontal Young's modulus versus horizontal compressive strength: (a) clay masonry; (b) calcium silicate masonry.

For both the clay and calcium silicate masonry, Figure 25 and Figure 26 depict the values of the vertical fracture energy versus the vertical compressive strength, and the horizontal fracture energy versus the horizontal compressive strength, respectively.

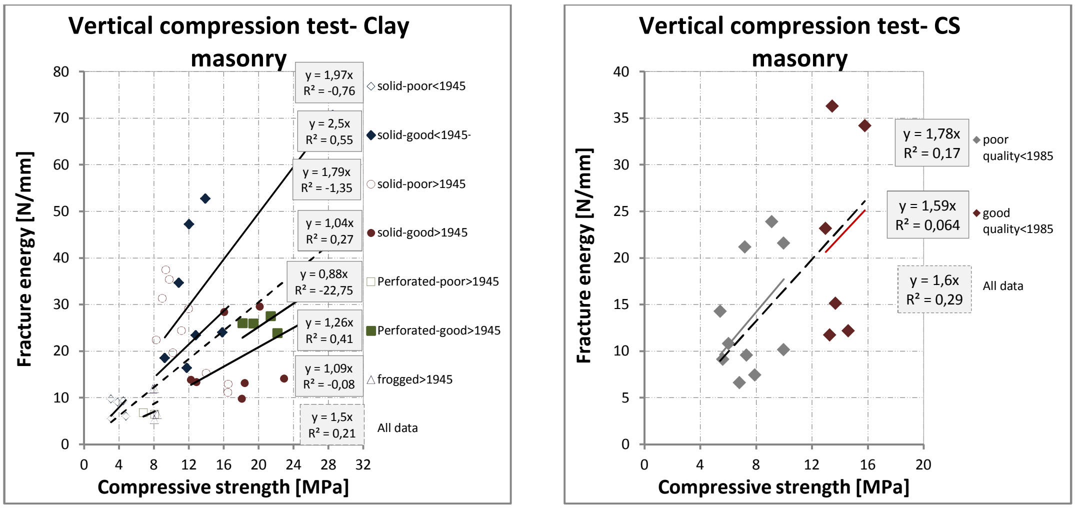

(a) (b)

Figure 25 – Vertical fracture energy versus vertical compressive strength: (a) clay masonry; (b) calcium silicate masonry.

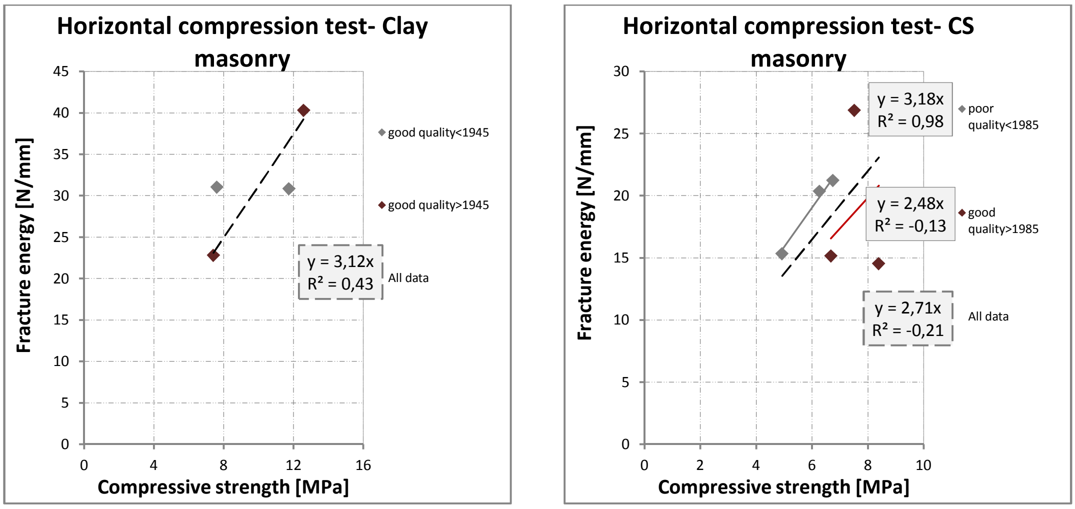

(a) (b)

Figure 26 – Horizontal fracture energy versus horizontal compressive strength: (a) clay masonry; (b) calcium silicate masonry.

Based on the communication in the project it was proposed to subdivide data into subdivisions. Table 6 indicates the mechanical properties of clay masonry subcategorised into the year of construction, type of the brick and quality, while Table 7 presents the mechanical properties of the calcium silicate masonry subcategorised into the year of construction and quality.

Table 6 - Overview of mechanical properties of clay brick masonry.

Material property	Symbol	Unit	Clay brick masonry																												
			(pre 1945)								(post 1945)																			
			Solid								Solid								Perforated								Frogged			
			Poor quality				Good quality				Poor quality				Good quality				Poor quality				Good quality				Poor quality			
			Average	Lower bound	Upper bound	C.o.V.	Average	Lower bound	Upper bound	C.o.V.	Average	Lower bound	Upper bound	C.o.V.	Average	Lower bound	Upper bound	C.o.V.	Average	Lower bound	Upper bound	C.o.V.	Average	Lower bound	Upper bound	C.o.V.	Average	Lower bound	Upper bound	C.o.V.
Flexural strength of masonry unit	$f_{mu,t}$	MPa	2.78	0.71	6.60	0.76	8.22	4.51	10.42	0.32	4.64	2.67	6.19	0.13	4.73	1.75	8.79	0.32	-	-	-	-	3.38	3.00	4.20	0.13	3.18	1.30	4.90	0.41
Compressive strength of masonry in the direction perpendicular to bed joints	$f_{m,v}$	MPa	3.95	3.09	4.79	0.01	13.45	8.50	32.40	0.17	11.25	8.29	16.54	0.22	21.32	12.27	28.60	0.30	6.88	4.50	8.80	0.20	20.74	18.17	26.26	0.12	7.95	7.35	8.40	0.04
Elastic chord modulus of masonry in the direction perpendicular to bed joints	$E_{m,v}$	GPa	2.63	1.27	4.05	0.51	9.36	3.34	19.92	0.48	5.68	2.21	8.80	0.22	11.34	6.99	15.60	0.23	3.85	1.50	5.70	0.36	8.69	6.72	11.33	0.20	2.57	1.20	3.87	0.38
Fracture energy in compression for loading perpendicular to bed joints	$G_{f-c,v}$	N/mm	8.18	5.53	9.72	0.23	36.50	16.40	70.64	0.52	24.60	11.06	37.37	0.27	22.92	9.72	33.63	0.41	6.59	6.44	6.74	0.03	27.19	23.82	32.92	0.13	8.87	5.29	11.96	0.40
Compressive strength of masonry in the direction parallel to bed joints	$f_{m,h}$	MPa	-	-	-	-	9.51	7.60	11.73	0.14	-	-	-	-	11.00	7.41	14.23	0.23	-	-	-	-	-	-	-	-	-	-	-	-
Elastic chord modulus of masonry in the direction parallel to bed joints	$E_{m,h}$	GPa	-	-	-	-	6.56	3.78	10.60	0.36	-	-	-	-	5.47	4.76	6.33	0.10	-	-	-	-	-	-	-	-	-	-	-	-
Fracture energy in compression for loading parallel to bed joints	$G_{f-c,h}$	N/mm	-	-	-	-	30.94	30.84	31.04	0.00	-	-	-	-	31.55	22.80	40.30	0.39	-	-	-	-	-	-	-	-	-	-	-	-
Average of compressive strength	f_m	MPa	3.95				11.48				11.25				16.16				6.88				20.74				7.95			
Average of elastic chord modulus	E_m	GPa	2.63				7.96				5.68				8.41				3.85				8.69				2.57			
Average of fracture energy	G_{f-c}	N/mm	8.18				33.72				24.60				27.24				6.59				27.19				8.87			
Masonry shear modulus	G_m	GPa	1.10				3.32				2.37				3.50				1.60				3.62				1.06			
Masonry bending strength with the moment vector parallel to the bed joints and in the plane of the wall	f_{x1}	MPa	-	-	-	-	-	-	-	-	-	-	-	-	-	-	-	-	0.33	0.26	0.42	0.20	-	-	-	-	-	-	-	-
Masonry bending strength with the moment vector orthogonal to the bed joint and in the plane of the wall	f_{x2}	MPa	-	-	-	-	0.83	0.55	1.28	0.47	1.20	0.59	1.68	0.13	1.24	0.76	1.58	0.03	0.92	0.88	0.99	0.05	0.87	0.81	0.96	0.10	-	-	-	-
Masonry bending strength with the moment vector orthogonal to the plane of the wall	f_{x3}	MPa	-	-	-	-	0.61	0.29	1.12	0.20	0.79	0.39	1.36	0.37	0.71	0.35	1.40	0.00	0.35	0.17	0.44	0.36	0.81	0.56	1.05	0.44	0.14	0.11	0.17	0.30
Masonry flexural bond strength between brick and mortar	$f_{b,bj}$	MPa	-	-	-	-	0.38	0.03	1.00	0.57	0.32	0.12	0.65	0.30	0.58	0.24	0.95	0.12	0.19	0.11	0.22	0.24	0.15	0.12	0.20	0.20	0.05	0.00	0.09	0.92
Masonry uniaxial bond strength between brick and mortar	f_b	MPa	-				0.25				0.21				0.39				0.13				0.10				0.03			
Masonry (bed joint) initial shear strength	f_{v0}	MPa	0.21	0.17	0.25	0.27	0.36	0.30	0.43	0.15	0.42	0.21	0.60	0.47	0.49	0.46	0.52	0.09	0.50	-	-	-	0.84	-	-	-	0.15	-	-	-
Masonry (bed joint) shear friction coefficient	μ	-	0.59	0.56	0.62	0.07	0.80	0.50	1.19	0.37	0.79	0.67	0.90	0.15	1.03	0.94	1.12	0.12	0.50	-	-	-	0.45	-	-	-	0.69	-	-	-
Fracture energy in shear	G_{f-s}	N/mm	-				0.33				-				0.93				-				-				-			
Fracture energy in tension	G_{f-t}	N/mm	0.035				0.035				0.035				0.035				0.035				0.035				0.035			

Table 7 - Overview of mechanical properties of calcium silicate brick masonry.

Material property	Symbol	Unit	Calcium Silicate (pre 1985) Poor quality Average	Poor quality Lower bound	Poor quality Upper bound	Poor quality C.o.V.	Good quality Average	Good quality Lower bound	Good quality Upper bound	Good quality C.o.V.
Flexural strength of masonry unit	$f_{mu,t}$	MPa	3.93	1.16	8.36	0.07	4.76	3.41	5.59	0.14
Compressive strength of masonry in the direction perpendicular to bed joints	$f_{m,v}$	MPa	8.00	5.42	11.97	0.19	13.89	12.97	15.78	0.03
Elastic chord modulus of masonry in the direction perpendicular to bed joints	$E_{m,v}$	GPa	6.35	2.48	10.00	0.23	9.22	8.27	11.48	0.01
Fracture energy in compression for loading perpendicular to bed joints	$G_{f\text{-}c,v}$	N/mm	14.15	6.60	23.87	0.44	25.38	11.73	36.27	0.55
Compressive strength of masonry in the direction parallel to bed joints	$f_{m,h}$	MPa	5.62	3.55	8.00	0.25	7.53	6.68	8.39	0.11
Elastic chord modulus of masonry in the direction parallel to bed joints	$E_{m,h}$	GPa	4.91	2.58	6.10	0.09	3.39	2.41	5.28	0.48
Fracture energy in compression for loading parallel to bed joints	$G_{f\text{-}c,h}$	N/mm	18.07	15.35	21.23	0.21	18.86	14.54	26.89	0.37
Average of compressive strength	f_m	MPa	6.81				10.71			
Average of elastic chord modulus	E_m	GPa	5.63				6.31			
Average of fracture energy	$G_{f\text{-}c}$	N/mm	16.11				22.12			
Masonry shear modulus	G_m	GPa	2.35				2.63			
Masonry bending strength with the moment vector parallel to the bed joints and in the plane of the wall	f_{x1}	MPa	0.13	0.00	0.28	0.12	-	-	-	-
Masonry bending strength with the moment vector orthogonal to the bed joint and in the plane of the wall	f_{x2}	MPa	0.59	0.59	0.59	-	-	-	-	-
Masonry bending strength with the moment vector orthogonal to the plane of the wall	f_{x3}	MPa	0.50	0.13	1.06	0.59	0.42	0.13	0.76	0.62
Masonry flexural bond strength between brick and mortar	$f_{b,bj}$	MPa	0.13	0.00	0.55	-	0.09	0.00	0.23	-
Masonry uniaxial bond strength between brick and mortar	f_b	MPa	0.08	0.00	0.37	0.76	0.06	0.00	0.15	0.67
Masonry (bed joint) initial shear strength	f_{v0}	MPa	0.29	0.18	0.40	0.31	0.28	0.03	0.53	0.89
Masonry (bed joint) shear friction coefficient	μ	-	0.76	0.70	0.85	0.07	0.82	0.53	1.10	0.49
Fracture energy in shear	$G_{f\text{-}s}$	N/mm	0.55				-			
Fracture energy in tension	$G_{f\text{-}t}$	N/mm	0.015				0.015			